JEE Journal of Ecological Engineering

Journal of Ecological Engineering, 2025, 26(8), 16–26
https://doi.org/10.12911/22998993/22998993/203520
ISSN 2299–8993, License CC-BY 4.0

Received: 2025.03.09
Accepted: 2025.05.26
Published: 2025.06.10

Bioreactor design for acidogenesis process of palm oil mill effluent

Arbie Saldi Zusri[1], Rivaldi Sidabutar[1,2], Irvan[1,2*], Bambang Trisakti[1,2], Michael Michael[1], Maya Sarah[1,2], Rondang Tambun[1,2]

[1] Department of Chemical Engineering, Faculty of Engineering, Universitas Sumatera Utara, Medan 20155, Indonesia
[2] Waste-to-Industrial Sustainable Energy Center, Universitas Sumatera Utara, Medan 20155, Indonesia
* Corresponding author's e-mail: irvan@usu.ac.id

ABSTRACT

Palm oil mill effluent (POME) is waste that can be used to produce biogas. One of the stages in the production of biogas from POME is the acidogenesis stage, where the products resulting from hydrolysis are further degraded into more specific organic products in the form of acetate, hydrogen, carbon dioxide, as well as intermediate products in the form of volatile fatty acids (VFA) such as propionate, butyrate, valerate, and its isoforms. This study aims to design an acidogenesis bioreactor to produce biogas from POME. The designed bioreactor is a stirred tank reactor with a volume of 1.000 L and operates on a batch system. The operating conditions for the acidogenesis process were a thermophilic temperature (55 °C), pH 5.5, and a substrate:starter ratio of 80%:20%. The bioreactor is constructed of stainless steel (SS SA-240 grade 304) due to its corrosion resistance and suitability for the acidic environment of POME, with a H/D ratio of 0.5/1 to 3/1. The mixer is a curved turbine impeller with six angles model A124, with a mixing speed of 0.46–1.29 rps and mixing power of 0.297–0.499 hp. The bioreactor is also equipped with control devices for the screening, feeding, and reaction stages. This bioreactor design supports a sustainable approach to POME management and renewable energy generation.

Keywords: acidogenesis, biogas, bioreactor, POME, thermophilic.

INTRODUCTION

Anaerobic digestion is a biochemical process without the presence of oxygen, which complex organic compounds are broken down by different types of anaerobic bacteria [1]. Four separate bacterial groups—hydrolysis, acidogenic, acetogenic, and methanogenic—are involved in this four-step process [2, 3]. Each of these microorganisms has unique physiological characteristics and dietary needs [4]. There will be an imbalance between the forms of acid and methane if all four groups of bacteria are operating under the same circumstances [5], which will result in a prolonged production period for biogas [6]. Many researchers divide the anaerobic digestion process into two steps as an effort to speed up the production of biogas [7]. The organic molecules in POME are first transformed into VFA compounds in the first stage by hydrolysis, acidogenesis, and acetogenesis (often referred to as the acidogenesis stage), and the VFA is then transformed into biogas in the second stage by methanogenesis [8].

As mentioned above, biogas production form POME involves four steps [9]. Specifically, at first, POME complex substances, such as lipids, proteins, and carbohydrates, are hydrolyzed by hydrolytic microbes and/or their enzymes into monomers such as fatty acids, amino acids, and sugars, respectively. The hydrolytic cycle generates a lot of organic waste and could experience rate restriction. Acidogenesis is the following process, which involves the breakdown of metabolic intermediaries including volatile fatty acids, alcohol, and aldehydes into acetate, carbon dioxide, and hydrogen gas. This process also known as fermentation process. Volatile fatty acids are produced by acidogenic bacteria and make up

the majority of these products. Along with the product produced during acidogenesis (acetate, carbon dioxide, and hydrogen gas), other compounds like ethanol, lactate, propionate, and butyrate are also produced in the third phase, known as acetogenesis. Methanogenesis, as last step in the biogas production, involves the acetotrophic and hydrogenotrophic bacterial groups. While acetotrophic methanogens employ formate as an electron donor for methane and carbon dioxide reduction, hydrogenotrophic methanogens use hydrogen as an electron acceptor for methane generation. Methanogenic bacteria may directly utilise the derivative of acetic acid, acetate, as a substrate to create biogas. While numerous studies have explored anaerobic digestion of various substrates, optimized bioreactor design for acidogenesis of POME under thermophilic conditions remains underexplored.

A bioreactor is simply described as a container with biological activity, such as microbes and enzymes, to produce high-value goods [10]. When it comes to the involvement of microbes in bioreactors, a mechanism should typically offer a biomechanical and biochemical environment that is expected to regulate nutrient and other compounds, such as how the gas is transferred to the microbes and their metabolism, so that high-value products are produced by the microbes [11]. To optimize growth and metabolic activity through the action of enzymes or microorganisms directly or indirectly to produce the desired product, such as biogas, a bioreactor's analysis and design should be carried out as an engineered device [12, 13]. When using nutrients as the building blocks for an ecosystem – which could be an organic or inorganic chemical compound or even a more sophisticated component – keep in mind that C and N levels or their ratio are frequently monitored [14]. Additionally, the end result of conversion may comprise primary metabolites and secondary metabolites as well as a consortium or single strain of microbes, starter cultures, enzyme, activators, etc. [15].

The two-stage anaerobic digestion process offers distinct advantages for POME treatment that address several inherent challenges of this complex waste stream. Unlike single-stage processes, the two-stage approach allows for more precise control of microbial populations and metabolic conditions in each stage [16], which is crucial for POME due to its high organic load and variable composition. By separating the process into distinct acidogenesis and methanogenesis stages, we can optimize conditions for each group of microorganisms, mitigating the potential process instabilities often encountered with POME. Specifically, the acidogenesis stage helps to hydrolyze and convert the complex organic compounds in POME into more readily metabolizable volatile fatty acids, reducing the potential for process inhibition and improving overall biogas yield [17]. This approach is particularly beneficial for POME, which contains high levels of lipids, proteins, and carbohydrates that require different enzymatic degradation strategies, thereby enhancing the overall efficiency of biogas production and waste treatment.

This study aims to design a bioreactor for POME's acidogenesis stage in biogas production. Before designing the bioreactor, biogas production has been conducted on a laboratory scale under thermophilic conditions. The resulting biogas was analyzed, and the operating conditions used on a laboratory scale were used as a reference in designing bioreactors. The bioreactor design includes calculation of bioreactor specifications, optimization of mixing speed and power consumption, and determination of necessary operating controls.

MATERIALS AND METHODS

Materials

Bioreactor design has begun with the production of biogas from POME on a laboratory scale. POME was collected from the fat pit of the Rambutan Mill, PTPN III, Indonesia. Fresh POME characteristics are shown in Table 1. Cow dung was employed as starter to provide microbial populations capable of degrading the substrate into biogas. The starter was obtained from an anaerobic digester at the biogas pilot plant at the Ecology Laboratory, Department of Chemical Engineering, Universitas Sumatera Utara. The acidogenesis takes place in a batch stirred tank fermenter (capacity 6 L), with a mixing speed of 250 rpm, pH of 5.5, thermophilic condition (55 °C), and a POME: starter ratio of 80%:20%. Acidogenesis was carried out in three stages: (1) screening, (2) feeding, (3) reaction, as shown in Figure 1. The screening process aims to filter out impurities or inorganic solids that cannot be degraded by acidogenic bacteria,

where the separation process is carried out using a screen and grit chamber. The feeding process includes the mixing of feed and starter, as well as the feeding them into bioreactor. To obtain a desired pH, $CaCO_3$ was added into bioreactor. The desired temperature was reached by the heating process slowly in the feeding process using a heating jacket medium.

Biogas production was monitored using a water displacement method. The displaced water volume was measured to quantify gas production. The biogas composition was analyzed using a gas chromatograph equipped with a thermal conductivity detector (GC-TCD) to determine the concentrations of methane (CH_4) and carbon dioxide (CO_2). Several key performance indicators were measured throughout the experiment includes volatile fatty acids (VFA), biogas yield, total solids (TS), volatile solids (VS), chemical oxygen demand (COD), and pH changes during the process. The total acidogenesis process was conducted over a period of 8.9 days, which was determined to be the optimal residence time based on preliminary studies. Samples were collected regularly to monitor the progression of the anaerobic digestion process and track the production of volatile fatty acids and biogas.

Overall, the stages of this bioreactor design are presented in Figure 2. In this work, bioreactor was designed with a capacity of 1000 L. Some of the assumptions used in the bioreactor design are as follows:

- There is no change in temperature during the reaction
- The stirring process occurs evenly throughout the bioreactor
- The product concentration at the start of the reaction is 0
- Inhibitors are considered minor or neglected

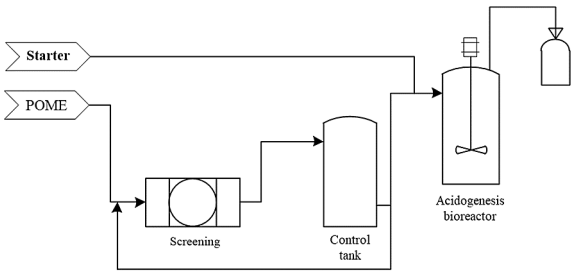

Figure 1. Schematic process of POME acidogenesis

The bioreactor was designed with stainless-steel (SS) SA-240 grade 304 material after carefully evaluating several alternative materials. While carbon steel offered lower initial costs, its significantly higher corrosion rate in acidic environments would require frequent replacement, potentially compromising reactor integrity. Duplex stainless steel provided superior corrosion resistance but at a substantially higher cost, making it economically impractical for large-scale applications [10, 11]. Polymer materials like polyethylene and fiberglass-reinforced plastic were also considered but were found to have limited temperature resistance and mechanical strength, particularly under the thermophilic conditions of the process. The selection of SS SA-240 grade 304 represented an optimal balance between corrosion resistance, mechanical properties, and economic considerations. The material can withstand corrosion at approximately 0.11 mm/year, and its proven performance in acidic and high-temperature environments made it the most suitable choice for the proposed bioreactor design [12, 13]. The reason for selecting this material remains its ability to withstand the process conditions running in acidic conditions which have the potential to cause corrosion in the reactor material, while also being relatively cost-effective and durable.

Table 1. Physicochemical characteristics of starter and fresh POME

Parameters	UoM	Starter	POME	Method/Instrument
TS	mg/L	60.000	13.420	APHA 2540B
VS	mg/L	56.000	10.520	APHA 2540E
TSS	mg/L	28.000	2.080	APHA 2540D
VSS	mg/L	26.000	1.920	APHA 2540E
pH	-	7.07	4.60	pH Meter
Alkalinity	mg/L	2.100	100	Titration
COD	mg/L	47.000	48.300	APHA 5220B

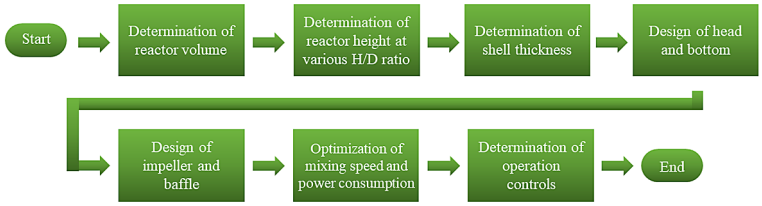

Figure 2. Schematic diagram of bioreactor design

RESULTS

Reactor volume

The total feed into the bioreactor was 1.000 L, consisting of 800 L of POME and 200 L of starter. In this work, the final reactor volume was increased by 20% of the total planned volume for safety factors, resulting in a final volume of 1.200 L.

Reactor height at various H/D ratio

The H/D ratio of bioreactor can vary between 1 and 3 [18]. In small-scale and laboratory-scale designs, the H/D = 1 is more often used. In larger designs, the H/D ratio up to 3 generally increases the retention time of gas bubbles in the bioreactor. It increases the heat exchange capacity of the bioreactor walls. Furthermore, Böhm et al. [19] explained that choosing a H/D ratio > 1 aims to reduce the shear effect of bursts of gas bubbles on the surface. Selecting the optimal H/D ratio involves balancing several factors, including gas retention time, mixing efficiency, and energy consumption. While a higher H/D ratio (> 1) improves gas retention and enhances heat exchange efficiency, it also increases the impeller diameter, leading to higher energy consumption for the drive motor. Conversely, a lower H/D ratio (≤ 1) reduces energy demand but may compromise mixing efficiency and gas retention [20]. Thus, an optimal H/D ratio should be selected based on the desired trade-off between energy efficiency and mixing performance, ensuring adequate substrate conversion while maintaining a feasible power requirement for agitation. In this work, we varied the H/D ratio of 0.5 to 3. Based on the calculation, the reactor height for the H/D ratios of 0.5, 1, 2, and 3 were 0.726 m, 1.152 m, 1.828 m, and 2.397 m; while the obtained ID were 1.452, 1.153, 0.914, and 0.799 m.

Shell thickness

The bioreactor was designed to be vertically cylindrical, with the shell volume calculation was carried out using Equation 1.

$$V_S = \frac{1}{4}\pi \times ID^2 \times H_s \quad (1)$$

where: Vs is shell volume in the form of total bioreactor volume, ID is inside diameter, and H_s is reactor height.

The fluid height in the bioreactor is a factor in determining the shell thickness. The fluid height in the bioreactor was set 80% of the shell height (H_s) by considering the safety factor. The final height of the fluid in the shell can be seen in Table 2. Operating pressure (P_{op}), hydrostatic pressure (P_{Hyd}), total pressure (P_{Tot}), and designed pressure (P_{Des}) also presented in Table 2. From Table 2, it can be seen that an increase in the H/D ratio causes an increase in the bioreactor shell pressure (total pressure and designed pressure). A high H/D ratio causes a smaller diameter so that the hydrostatic pressure becomes higher. As a result, the shell pressure also increases.

Table 2. Fluid height, pressure and reactor diameter at various H/D ratio

H/D ratio	Fluid height (m)	ID (m)	OD (m)	P_{Op} (Psia)	P_{Hyd} (Psia)	P_{Tot} (Psia)	P_{Des} (Psia)
0.5	0.581	1.452	1.468	14.700	0.903	15.603	17.163
1	0.922	1.153	1.169		1.434	16.134	17.747
2	1.464	0.914	0.931		2.276	16.976	18.673
3	1.918	0.799	0.815		2.982	17.682	19.450

After obtaining the pressure value in the bioreactor, the shell thickness was calculated using Equation 2:

$$t_s = \frac{P \times r_i}{f \times E - 0.6P} + C \quad (2)$$

where: t_s is the shell thickness, P is the design pressure, f is favorable stress, r_i is the shell radius, and C is the material corrosion factor (0.125 in/year). Based on the the calculation, it was found that the shell thickness H/D ratios of 0.5, 1, 2, and 3 were 0.473 m, 0.456 m, 0.443 m, and 0.437 m. An increase in shell pressure causes a decrease in shell thickness. This could be due to the addition of the radius value to the shell with a smaller H/D ratio requiring a material with a larger thickness. The outer diameter (OD) value is obtained by adding the ID value twice the shell thickness.

Head and bottom design

The designed bioreactor uses thorisperical head and bottom. Torispherical has a larger surface area compared to elliptical and hemispherical designs. Calculation of head and bottom thickness was performed using the Equation 3:

$$t_h = \frac{P \times r_c \times W}{(2 \times f \times E) - (0.2P)} + C \quad (3)$$

After obtaining the wall thickness, the head height can be obtained using the Equation 4–9:

$$a = \frac{ID}{2} \quad (4)$$

$$AB = a - icr \quad (5)$$

$$BC = rc - icr \quad (6)$$

$$AC = \sqrt{(BC)^2 - (AB)^2} \quad (7)$$

$$b = rc - AC \quad (8)$$

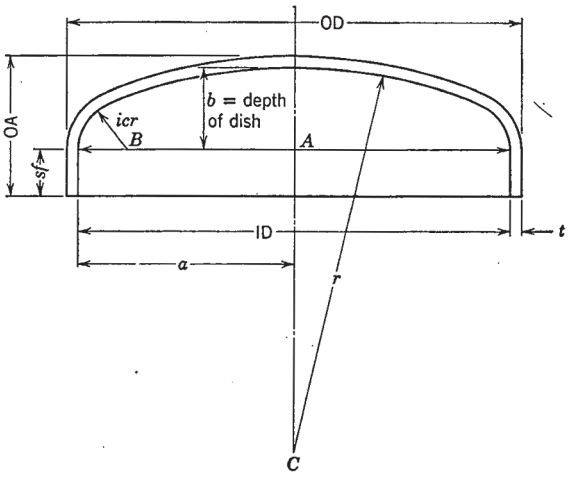

Figure 3. Schematic of torispherical head

$$OA = th + b + sf \quad (9)$$

where: a, AB, BC, AC and b represent parts of the head reactor as shown in Figure 3. The head height, total bioreactor height, and bioreactor surface area can be seen in Table 3.

Impeller and baffle design

In designing this stirrer system, the first thing to do is determine the type of impeller that will be used in the process. In this work, we have chosen a curved turbine impeller with six angles model A124. The reasons for choosing this impeller include: (i) this type of impeller is useful for a wide range of viscosities, and (ii) it is commonly used for mixing solutions including slurries. The impeller diameter (D_i) was calculated by dividing the reactor diameter (ID) by 3. The height (t_b) and width (W_b) of the impeller blades is obtained by multiplying Di by 0.2 and 0.25, respectively.

In this stirred tank reactors design, four baffles are employed for disrupting swirling motion and improve fluid circulation, which is crucial for maintaining homogeneity in the substrate mixture. Using fewer than four baffles (e.g., two or three) can result in incomplete mixing and the

Table 3. Head height, total height, and surface area of bioreactor at various H/D ratio

H/D ratio	Shell height (m)	Head height (m)	Total height (m)	Surface area (m^2)
0.5	0.726	0.793	2.313	18.663
1	1.153	0.644	4.746	18.526
2	1.830	0.526	2.881	20.537
3	2.398	0.468	3.334	23.016

formation of dead zones, leading to uneven substrate processing. Higher number of baffles beyond four may cause excessive turbulence and increase power consumption without significant improvements in mixing performance [20, 21]. Therefore, four baffles were selected as the configuration to ensure an effective balance between mixing efficiency and energy requirements. The baffle width was calculated by dividing the ID by 12. The specification of impeller and baffle can be seen in Table 4.

The calculation of the required amount of impeller was carried out by dividing the value of the Water Equivalent Liquid High (WELH) by the height of the bioreactor. WELH is the height of the fluid in the reactor multiplied by the specific gravity of the fluid. Based on the calculation, the required amount of impeller for each H/D ratio of 0.5, 1, 2, and 3 was 1, 1, 1, and 2. An increase in the H/D ratio causes an increase in the number of impellers required.

Mixing speed and power consumption

The power requirement for the impeller is influenced by two factors, namely the Reynolds number (N_{Re}) and the power number (N_P). N_{Re} can be calculated using the Equation 10, while N_P can be obtained using Equation 11:

$N_{Re} =$ Please, Correct equation (10)

$$N_P = \frac{P}{\rho \times n^3 \times Di^5} \quad (11)$$

where: n is the mixing speed, Di is the impeller diameter, ρ is the fluid density, μ is the fluid viscosity, and P is the mixing power (hp). The value of n was calculated using a trial by determining the P value.

The initial mixing power was calculated using a value of 10 hp/1000 gallons, resulting in power required for 1.200 L was 0.317 hp. The mixing power value is substituted into Equation 10 to get the N_{Re} value, then the obtained value was used to get the NP value on the N_P vs N_{Re} graph. The validation was carried out for the n value using equation 11. The $N_{Re,}$ n, and N_P values for each H/D ratio can be seen in Table 5, and the relationship between H/D ratio and mixing power is presented in Figure 4.

In Figure 4, mixing power is controlled constant, it can be seen that the number power decreases as the H/D ratio increases. From these results, it can be obtained that the streamlined tank geometry requires lower number power. The power requirements at the H/D ratios of 2 and 3 are not much different, but the increase in the H/D ratios of 0.5 and 1 increases the need for high number. The geometric shape of the reactor tank with a high H/D ratio causes a decrease in the agitator power requirements.

Control operation

The acidogenesis process involves organic compounds degradation into simpler components with fermentative bacteria. In general, two bacteria play an essential role in the acidogenesis stage, namely *Clostridia* and bacteria from the *Bacteroicideae* family. Both types of bacteria can survive in extreme conditions, namely at high temperatures and low pH. As previously mentioned, the acidogenesis process consist of three stages: screening, feeding, and reaction. The operation control system at each stage must be carried out to ensure that each parameter follows the standards set. The operational control system includes measuring feed and product quality and process indicators such as pH, temperature, and processing time. The measurement process is carried out manually or recorded through instruments periodically.

Table 6 displays monitoring points and the frequency of observations at each stage. In this work, pH is set to 5.5. According to Ahmed et al. [21], the pH of POME is 3.4–5.2. Table 6 also shows the quality of the raw materials fed into

Table 4. Head, bottom and impeller diameter

H/D ratio	Impeller diameter (m)	Offset bottom (m)	Offset top (m)	Baffle thick (m)	Blade thick (m)	Blade height (m)
0.5	0.363	0.182	0.015	0.073	0.091	0.073
1	0.288	0.144	0.012	0.058	0.072	0.058
2	0.229	0.114	0.006	0.046	0.057	0.046
3	0.200	0.100	0.008	0.040	0.050	0.040

Table 5. Reynold number and power consumption

H/D ratio	N_{Re}	n (rps)	Mixing power (hp)
0.5	918.225	0.043	0.316
1	918.819	0.066	0.316
2	919.108	0.105	0.316
3	918.762	0.266	0.316

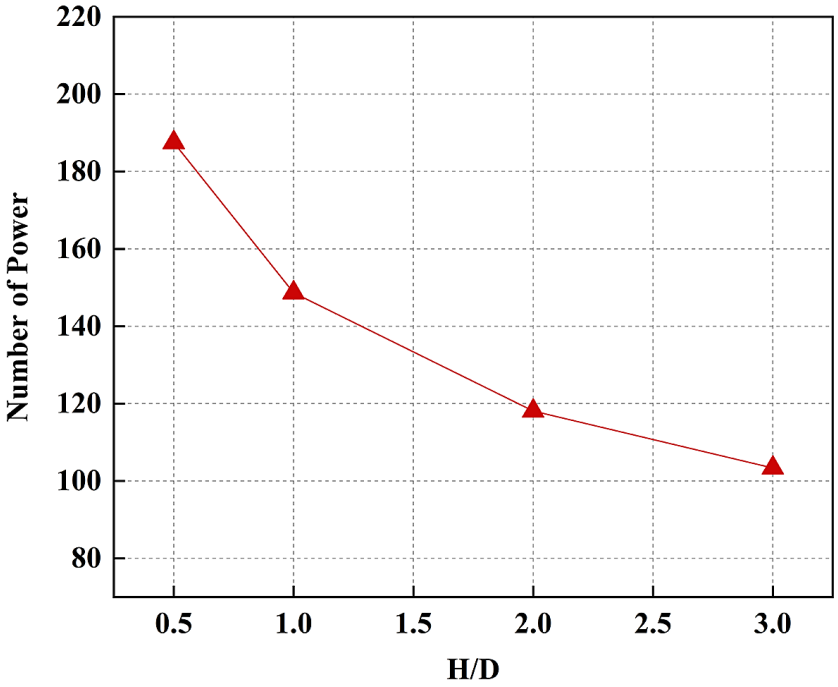

Figure 4. H/D ratio vs. number of bioreactor power

the reactor. Analysis of the raw materials quality is carried out in the feeding process based on predetermined quality standards. The recirculation process from the bioreactor to the balance tank is carried out if the raw materials quality exceeds the set standards.

Operation control for screening process

The screening process aims to filter impurities or inorganic solids that acidogenic bacteria cannot degrade. Separating inorganic solids at the screening stage also aims to avoid damage to the pump and accumulation in the bioreactor. The screening process is carried out using a screen and a grit chamber. The control process is carried out through POME flow rate and filtering loads. The control process is carried out once a day, and the maintenance/cleaning process on the screen is carried out after one process cycle to ensure that there is no buildup on the screen.

Operation control for feeding process

In this design, the residence time for each cycle was 8.9 days, so the total feeding time required was 4.45 days. Flow rate control was carried out once/hour with a flow rate of 7.5 L/hour for feed and 1.9 L/hour for starter. The heating process in the bioreactor is carried out before mixing takes place with a temperature range of 55 °C. Heating control is carried out automatically with a control valve with monitoring for one time/hour.

Operation control for reaction process

In the reaction process, sample quality was measured by analysis of TS, TSS, VS, VSS, and alkalinity for once/day, and analysis of COD, SCOD, and VFA was carried out twice/day. pH observations were carried out for once/4 hours by adding calcium bicarbonate as a pH control. Operating temperature control is carried out automatically using a control valve with monitoring for one time/hour.

Table 6. Monitoring and frequency of operating control on every stages

Parameter	Unit	Monitoring frequency	Method	Control operation	Ref.
Screening process					
Flow rate	L/s	day	-	-	-
Screening volume	m^3/day	day	-	50 L sand/1000 m^3 POME	[22]
Feeding process					
Feed flow rate	L/hour	hour	-	-	-
Starter flow rate	L/hour	hour	-	-	-
Temperature	°C	hour	-	-	-
pH	-	cycle	-	-	-
TS	mg/L	cycle	APHA 2540B	11,500–79,000	[23]
TSS	mg/L	cycle	APHA 2540D	5.000–54,000	[23]
VS	mg/L	cycle	APHA 2540E	9.000–72,000	[23]
VSS	mg/L	cycle	APHA 2540E	-	
COD	mg/L	cycle	APHA 5520C	15,000–100,000	[23]
Reaction Process					
Temperature	°C	hour	-	Min. 55 °C	[22]
pH	-	4 hours	APHA 4500H	5–5.5	[22]
Cycle time	Day	cycle	-	-	-
VFA	mg/L	2 days	APHA 5560B	Min 4.500 mg/L	[24]
TSS	mg/L	day	APHA 2540D	-	-
VSS	mg/L	day	APHA 2540E	-	-
COD	mg/L	2 days	APHA 5520C	-	-
Biogas quality	-	day	-	-	-
Alkalinity	mg/L	day	-	-	-
TS	mg/L	day	APHA 2540B	-	-
TVS	mg/L	day	-	-	-

DISCUSSION

The designed acidogenesis bioreactor for biogas production from POME represents a significant advancement in waste-to-energy technologies, particularly in the context of palm oil mill effluent management. POME, a byproduct of palm oil production, poses environmental challenges due to its high organic load. Utilizing it for biogas production mitigates its environmental impact and provides a renewable energy source.

Significance of the findings

This study focused on optimizing the acidogenesis stage, a critical phase in anaerobic digestion, where complex organic molecules are converted into volatile fatty acids (VFA), acetate, hydrogen, and carbon dioxide. One of the key findings is the effect of the H/D ratio on reactor performance. The results demonstrated that while higher H/D ratios improved gas retention and heat exchange, they also increased energy demand for mixing. These findings align with those of Ahmad et al. [27], who reported that a higher H/D ratio reduces the shear effect of gas bubbles but requires higher power input for agitation. The balance between these factors is crucial in large-scale applications, where operational costs play a significant role.

Additionally, the selection of four baffles was justified by its role in preventing vortex formation and improving mixing efficiency. Prior studies, such as those by Wang et al. [28], have demonstrated that reducing the number of baffles leads to dead zones, whereas increasing baffles beyond four does not significantly enhance mixing but results in excessive turbulence and power consumption. The curved turbine impeller (model A124) was also chosen for its efficiency across a range of viscosities, particularly in fermentative processes involving slurries. Incorporating impeller with six angles ensured effective mixing,

crucial for maintaining homogeneity in the bioreactor. The impeller's specifications, determined through detailed calculations, were designed to handle the substrate's varying viscosities. Operational control was a significant focus, with stringent monitoring of parameters such as pH, temperature, and mixing speed. This ensured that the bioreactor operated within the optimal conditions identified in the laboratory. Regular quality checks and adjustments, particularly during the screening, feeding, and reaction stages, were essential for maintaining process stability and maximizing biogas yield.

Compared to previous studies on POME acidogenesis, this study introduces a more systematic approach to reactor design by integrating key parameters such as impeller speed, baffle configuration, and material selection. For instance, Trisakti et al. [8] focused on optimizing pH and retention time but did not extensively examine the mechanical aspects of reactor design. Our study builds upon this by incorporating a mechanical and structural optimization perspective, ensuring that both microbial and engineering considerations are addressed. Another relevant study by Rezapoor and Rahimpour [29] explored various bioreactor configurations for POME treatment but primarily focused on process efficiency rather than design optimization. Their findings indicated that two-stage anaerobic digestion improves biogas yield; however, they did not analyze the influence of H/D ratio, impeller selection, or energy consumption, which are addressed in our study. By incorporating these additional factors, our research provides a more holistic approach to bioreactor design for acidogenesis.

Potential benefits and challenges of real-world applications

The practical application of this bioreactor design in industrial settings offers several benefits and challenges that must be considered before large-scale implementation. The modular design of the bioreactor allows for easy scaling from laboratory to industrial applications. Since the process parameters were optimized based on laboratory-scale trials, future pilot-scale experiments should validate how effectively these conditions translate to larger systems. A major advantage of the stirred tank reactor design is its adaptability as multiple units can be installed in parallel to accommodate varying POME volumes. However, scaling up introduces challenges such as maintaining consistent mixing efficiency and heat transfer across larger volumes. The increased reactor size could also lead to fluctuations in pH, temperature, and substrate concentration, potentially affecting microbial activity. Computational fluid dynamics (CFD) simulations or pilot-scale studies should be conducted to assess these effects before full-scale deployment.

The use of SS SA-240 grade 304 ensures durability and resistance to the acidic conditions of POME digestion, reducing long-term maintenance costs. Compared to alternative materials like carbon steel, which is cheaper but prone to corrosion, stainless steel offers a more cost-effective long-term investment. However, initial capital costs remain a challenge, especially for small and medium-scale palm oil mills. The combination of stainless-steel construction and mechanical stirring components increases upfront costs compared to simpler passive bioreactors such as anaerobic lagoons or covered digesters. Future cost analyses should explore hybrid approaches, such as integrating lower-cost materials in non-critical components to reduce capital expenditures. Additionally, energy consumption for mixing and heating is another cost factor. While our results show that an H/D ratio of 2–3 minimizes power consumption, alternative low-energy mixing strategies (e.g., gas recirculation, mechanical agitation optimization) should be explored for industrial-scale applications.

This bioreactor design requires continuous monitoring and control of key parameters, including: pH control (maintained at 5.5 using calcium bicarbonate), temperature regulation (thermophilic range of 55 °C), and mixing power and impeller speed optimization. Automating these controls via sensor-based monitoring systems could enhance process stability and reduce labor costs. However, integrating such automation adds technical complexity and cost, requiring trained personnel for maintenance. Additionally, variability in POME composition across different palm oil mills could affect bioreactor performance. Real-world application would require periodic feedstock analysis and potential adjustments to process conditions to maintain efficiency.

Limitations and future research

Despite the promising results, some limitations must be acknowledged. First, this study was based

on batch operation, which differs from continuous operation commonly used in industrial biogas production. Future studies should explore how these design parameters perform under continuous feeding conditions, which may introduce variations in microbial activity and process stability. Second, the energy consumption of the mixing system needs further evaluation, particularly in terms of optimizing impeller speed to balance power requirements with biogas yield. CFD simulations could provide deeper insights into flow patterns and mixing efficiency. Finally, the bioreactor's performance should be tested on a larger scale to assess its feasibility in industrial applications.

Overall, this study provides valuable insights into the design and optimization of an acidogenesis bioreactor for POME treatment. By addressing mechanical, biochemical, and operational factors, the findings contribute to a more efficient and sustainable approach to biogas production. Future research should focus on scalability, automation, and cost-benefit analysis to facilitate industrial implementation.

CONCLUSIONS

The design and development of an acidogenesis bioreactor for biogas production from POME highlight the potential of converting a problematic waste stream into a valuable energy resource. The study successfully identified optimal conditions for the acidogenesis stage – thermophilic temperature (55 °C), pH 5.5, and a substrate: starter ratio of 80%:20% – crucial for effective biogas production. Key aspects of the bioreactor design, such as selecting a stirred tank reactor with a 1.000 L volume and construction from corrosion-resistant stainless steel (SS SA-240 grade 304), ensured the system's durability and efficiency. Carefully considering the H/D ratio, impeller type, and mixing speed demonstrated the importance of balancing gas retention, heat exchange efficiency, and energy consumption. A curved turbine impeller with six angles and four baffles ensured effective mixing and homogeneity within the bioreactor, critical for optimal microbial activity and substrate conversion.

Operational controls, including regular monitoring and adjustments of pH, temperature, and feed quality, were essential for maintaining the bioreactor's performance. The detailed monitoring framework ensured the bioreactor operated within the desired parameters, thus maximizing biogas yield and process stability. This study provides a comprehensive framework for designing an acidogenesis bioreactor, offering valuable insights into optimizing biogas production from POME. The results demonstrate the feasibility and effectiveness of the proposed design, contributing to sustainable waste management and renewable energy generation. Future work may focus on scaling up the bioreactor design and exploring its applicability to other types of organic waste, further enhancing its environmental and economic impact.

REFERENCES

1. Dwivedi N. (2024). A comprehensive study on anaerobic digestion of organic solid waste: A review on configurations, operating parameters, techno-economic analysis and current trends, *Biotechnology Notes, 5*, 33–49, doi: 10.1016/j.biotno.2024.02.001.
2. Tsigkou K., Zagklis D., Parasoglou M., Zafiri C., and Kornaros M. (2022). Proposed protocol for rate-limiting step determination during anaerobic digestion of complex substrates, *Bioresource Technology, 361*, 127660, doi: 10.1016/j.biortech.2022.127660.
3. Lim J. W., Park T., Tong Y. W., and Yu Z. (2020). *Chapter One - The microbiome driving anaerobic digestion and microbial analysis*, in Advances in Bioenergy, 5, Y. Li and S. K. Khanal, Eds., Elsevier, 1–61. doi: 10.1016/bs.aibe.2020.04.001.
4. El Asri O. (2023). *Anaerobic Biodegradation: The Anaerobic Digestion Process*, in Handbook of Biodegradable Materials, G. A. M. Ali and A. S. H. Makhlouf, Eds., Cham: Springer International Publishing, 85–110. doi: 10.1007/978-3-031-09710-2_4.
5. Schink B. and Stams A. J. M. (2013). *Syntrophism Among Prokaryotes*, in The Prokaryotes: Prokaryotic Communities and Ecophysiology, E. Rosenberg, E. F. DeLong, S. Lory, E. Stackebrandt, and F. Thompson, Eds., Berlin, Heidelberg: Springer, 471–493. doi: 10.1007/978-3-642-30123-0_59.
6. Jiang M., Qiao W., Wang Y., Zou T., Lin M., and Dong R. (2022). Balancing acidogenesis and methanogenesis metabolism in thermophilic anaerobic digestion of food waste under a high loading rate, *Science of The Total Environment, 824*, 153867, doi: 10.1016/j.scitotenv.2022.153867.
7. Rajendran K., Mahapatra D., Venkatraman A. V., Muthuswamy S., and Pugazhendhi A. (2020). Advancing anaerobic digestion through two-stage processes: Current developments and future trends, *Renewable and Sustainable Energy Reviews, 123*, 109746, doi: 10.1016/j.rser.2020.109746.
8. Trisakti B., Manalu V., Taslim I., and Turmuzi M.

(2015). Acidogenesis of palm oil mill effluent to produce biogas: effect of hydraulic retention time and pH, *Procedia - Social and Behavioral Sciences*, *195*, 2466–2474, doi: 10.1016/j.sbspro.2015.06.293.

9. Garritano A. N., de O. Faber M., De Sá L. R. V., and Ferreira-Leitão V. S. (2018). Palm oil mill effluent (POME) as raw material for biohydrogen and methane production via dark fermentation, *Renewable and Sustainable Energy Reviews, 92*, 676–684, doi: 10.1016/j.rser.2018.04.031.
10. Delavar M. A. and Wang J. (2022). *Chapter 7 - Bioreactor concepts, types, and modeling*, in Advanced Methods and Mathematical Modeling of Biofilms, M. A. Delavar and J. Wang, Eds., Academic Press, 195–245. doi: 10.1016/B978-0-323-85690-4.00004-X.
11. Pan J., Lacroix D., Zhou Y., and Wang B. (2023). Editorial: Biomechanical and biochemical regulation of the musculoskeletal system, *Front Bioeng Biotechnol, 11*, 1192638, doi: 10.3389/fbioe.2023.1192638.
12. Liew Y. X., et al. (2020). Enzymatic pretreatment to enhance anaerobic bioconversion of high strength wastewater to biogas: A review, *Sci Total Environ, 713*, 136373, doi: 10.1016/j.scitotenv.2019.136373.
13. Jameel M. K. et al. (2024). Biogas: Production, properties, applications, economic and challenges: A review, *Results in Chemistry, 7*, 101549, doi: 10.1016/j.rechem.2024.101549.
14. Kitadai N. and Maruyama S. (2018). Origins of building blocks of life: A review, *Geoscience Frontiers*, *9*(4), 1117–1153, doi: 10.1016/j.gsf.2017.07.007.
15. Prasetyo J., Senda S. P., Wulandari W., and Anindita N. N. (2020). Bio-CSTR for Biogas Production from POME Treatment - Technology: Design and Analysis, in *AIP Conference Proceedings*, doi: 10.1063/5.0000783.
16. Morales-Polo C., Cledera-Castro M. D. M., and Moratilla Soria B. Y. (2018). Reviewing the anaerobic digestion of food waste: from waste generation and anaerobic process to its perspectives, *Applied Sciences, 8*(10), Art. no. 10, doi: 10.3390/app8101804.
17. Nagarajan S., Jones R. J., Oram L., Massanet-Nicolau J., and Guwy A. (2022). Intensification of acidogenic fermentation for the production of biohydrogen and volatile fatty acids—a perspective, *Fermentation, 8*(7), Art. no. 7, doi: 10.3390/fermentation8070325.
18. Doran P. M. (1995). *Bioprocess Engineering Principles*. doi: 10.1016/b978-0-12-220855-3.x5000-7.
19. Böhm L., Hohl L., Bliatsiou C., and Kraume M. (2019). multiphase stirred tank bioreactors – new geometrical concepts and scale-up approaches, *Chemie-Ingenieur-Technik*, *91*(12), 1724–1746, doi: 10.1002/cite.201900165.
20. Christwardana M., Harvianto G. R., Sunandar K., Novian W. D., and Ramanto R. (2021). Effect of H/D ratio and impeller type on power consumption of agitator in continuous stirred tank reactor for nitrocellulose production from cotton linter and nitric acid, *International Journal of Chemical Reactor Engineering*, *18*(12), 1–12, doi: 10.1515/ijcre-2020-0109.
21. Ahmed Y., Yaakob Z., Akhtar P., and Sopian K. (2015). Production of biogas and performance evaluation of existing treatment processes in palm oil mill effluent (POME), *Renewable and Sustainable Energy Reviews*, *42*, 1260–1278, doi: 10.1016/j.rser.2014.10.073.
22. de Lemos Chernicharo C. A. (2015). Anaerobic Reactors, in *Biological Waswater Treatment Series*, *4*, London: IWA Publishing, doi: 10.2166/9781780402116.
23. Ahmed Y., Yaakob Z., Akhtar P., and Sopian K. (2015). Production of biogas and performance evaluation of existing treatment processes in palm oil mill effluent (POME), *Renewable and Sustainable Energy Reviews*, *42*, 1260–1278, doi: 10.1016/j.rser.2014.10.073.
24. Pind P. F., Angelidaki I., Ahring B. K., Stamatelatou K., and Lyberatos G. (2003). Monitoring and Control of Anaerobic Reactors, in *Advances in Biochemical Engineering/bBotechnology*, *82*, Berlin: Springer-Verlag, 135–182. doi: 10.1007/3-540-45838-7_4.
25. Zaiat M., Rodrigues J. A. D., Ratusznei S. M., De Camargo E. F. M., and Borzani W. (2001). Anaerobic sequencing batch reactors for wastewater treatment: A developing technology, *Applied Microbiology and Biotechnology*, *55*(1), 29–35. doi: 10.1007/s002530000475.
26. Jaibiba P., Vignesh S. N., and Hariharan S. (2020). Working principle of typical bioreactors, in *Bioreactors: Sustainable Design and Industrial Applications in Mitigation of GHG Emissions*, Elsevier Inc., ch. 10, 145–173. doi: 10.1016/B978-0-12-821264-6.00010-3.
27. Ahmad A., Ghufran R., and Abd. Wahid Z. (2011). Bioenergy from anaerobic degradation of lipids in palm oil mill effluent, *Rev Environ Sci Biotechnol, 10*(4), 353–376, doi: 10.1007/s11157-011-9253-8.
28. Wang C., et al. (2022). A review on the hydrothermal treatment of food waste: processing and applications, *Processes, 10*(11), Art. no. 11, doi: 10.3390/pr10112439.
29. Rezapoor P. and Rahimpour M. R. (2023). Animal waste to energy, technologies, economics, and challenges, in *Reference Module in Earth Systems and Environmental Sciences, Elsevier*. doi: 10.1016/B978-0-323-93940-9.00148-1.